

Topological quantum phase transition in bond-alternating spin-1/2 Heisenberg chains

Hai Tao Wang,¹ Bo Li,¹ and Sam Young Cho^{1,*}

¹Centre for Modern Physics and Department of Physics,
Chongqing University, Chongqing 400044, The People's Republic of China

We investigate string correlations in an infinite-size spin-1/2 bond-alternating Heisenberg chain. By employing the infinite matrix product state representation with the infinite time evolving block decimation method, a finite string correlation for extremely large lattice distances is *directly* observed, contrast to an extrapolated extreme value for finite size chains. We find that a topological quantum phase transition occurs between two different phases separated and characterized by two different long-range string orders in the space of bond-alternating interactions. Also, the critical exponent β from the long-range string orders is obtained as $\beta = 1/12$ and the central charge at the critical point is obtained as $c \approx 1$, which shows that the topological phase transition belongs to the Gaussian universality class. In addition, it is shown that, for the topological quantum phase transition, the phase boundary can be captured by the singular behavior of the von Neumann entropy and the pinch point of the fidelity per site.

PACS numbers: 75.10.Pq, 03.65.Vf, 03.67. Mn, 64.70.Tg

I. INTRODUCTION

Landau's symmetry breaking theory¹ (LSBT) for understanding the continuous phase transitions is one of the cornerstone theories in quantum many-body systems. Most phases and phase transitions could be understood by a local order parameter characterizing a symmetry breaking^{2,3}. Recently, a new type of phase transitions, for instance, appearing in the discovery of the quantum Hall effect⁴, could not be understood well by local order parameters. Such quantum phase transitions seem to occur between two different phases without any explicit symmetry breaking. A non-local order, i.e., a so-called topological order⁵, rather than local orders, enables us to characterize the two phases. The quantum phase transition is called topological quantum phase transitions (TQPTs)⁶⁻¹⁴. Topological orders have been intensively studied in various systems such as fractional quantum Hall states^{15,16}, Haldane phase¹⁷, chiral spin liquids^{18,19}, Z_2 spin liquids²⁰⁻²², and so on.

In spin lattice systems, especially, a string order as a prototype example of non-local long-range order was introduced by Nijs and Rommelse²³, and Tasaki²⁴ and characterizes the Haldane phase. Since then, non-local string orders have been extensively applied to study quantum phase transitions in various spin systems such as anisotropic spin-1 Heisenberg chains²⁵, frustrated antiferromagnetic Heisenberg spin chains²⁶, spin-1/2^{27,28} and spin-1²⁹ alternating Heisenberg chains, XXZ spin-1 chain³⁰, spin ladders^{31,32}, spin tubes³³, and Kitaev spin model^{11,12}, and so on. Also, a TQPT has been shown between two phases respectively characterized by different non-local string (topological) order parameters in Kitaev spin models^{11,12}.

In this paper, we study a TQPT in an infinite spin-1/2 bond-alternating Heisenberg chain by introducing two non-local string orders. To compute the two long-range string orders, we employ the infinite matrix product state (iMPS) representation^{34,35} with the infinite time evolving block decimation (iTEBD) method developed by Vidal³⁵. Compared to finite-size lattice systems where a long-range order determined by an extrapolated value of correlations, the iMPS approach al-

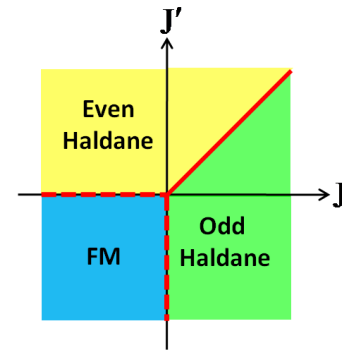


FIG. 1: (Color online) Ground state phase diagram for the spin-1/2 bond-alternating Heisenberg chain in the plane of the bond alternations J and J' . The even- and odd-Haldane phases are denoted by yellow and green, respectively. The ferromagnetic phase occurs in the blue region. Note that the red solid line between the two Haldane phases denotes a continuous phase transition corresponding to the topological phase transition, while the red dashed lines indicate a discontinuous phase transition.

lows us to calculate non-local long-range orders³⁰ directly. The string correlations and the dimer correlations directly calculated from the iMPS groundstate show clearly that there are two topologically ordered phases characterized by two long-range string orders. From the topological characterization, we find that there are three phases including the ferromagnetic phase in the spin-1/2 bond-alternating Heisenberg chain (See Fig. 1). Furthermore, the central charge $c \approx 1$ at the phase boundary between the two topologically ordered phases and the critical exponent of the string orders $\beta = 1/12$ show that the TQPT belongs to Gaussian-type phase transition. We discuss that the von Neumann entropy and the fidelity per lattice site (FLS) can capture the TQPT.

This paper is organized as follows. In Sec.II, we introduce the spin-1/2 alternating Heisenberg chain model and discuss its groundstate energy. Section III devotes to discuss the topological phase transition by means of the comparison between the odd-/even-string correlations and the dimer correlations.

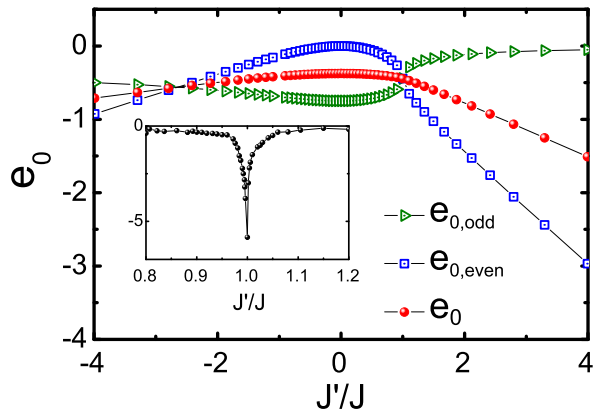


FIG. 2: (Color online) Ground state energy per site e_0 and the odd/even-bond energies $e_{0,even/odd}$ as a function of J' with $J = 1$. In the inset, the second order derivative of energy per site is plotted around the critical point $J' = J = 1$.

In Sec. IV, the phase transitions are discussed from the von Neumann entropy. The TQPT is classified based on the central charge via the finite-entanglement scaling. The FLS is discussed to detect the TQPT in Sec. V. Finally, our conclusion is given in Sec. VI.

II. SPIN-1/2 ALTERNATING HEISENBERG CHAIN AND GROUNDSTATE ENERGY

The spin-1/2 alternating Heisenberg chains are described by the Hamiltonian^{27,36,37}

$$H = \sum_i (J \vec{S}_{2i-1} \cdot \vec{S}_{2i} + J' \vec{S}_{2i} \cdot \vec{S}_{2i+1}), \quad (1)$$

where $\vec{S} = (S^x, S^y, S^z)$ are the spin-1/2 operators. J and J' are two alternative nearest-neighbor exchange couplings. In order to cover the whole range of the parameter J and J' , we take $J = \cos \theta$, $J' = \sin \theta$. For $\theta = \pi/4$, this model is reduced to the conventional antiferromagnetic (AF) isotropic Heisenberg chain with being gapless, while for $\theta = 0$ or $\pi/2$, the system will be characterized by decoupled singlets. When θ approaches the limit $\theta = -\pi/2$ from $\theta = 0$, Eq. (1) can be regarded effectively as a $S = 1$ AF isotropic Heisenberg chain, which can be characterized by a gapful Haldane phase.

From our iMPS groundstate in the Hamiltonian of Eq. (1), one can calculate the groundstate energy. In Fig 2, the groundstate energy per site e_0 , as an average value of the energies for odd bond $e_{0,odd}$ and even bond $e_{0,even}$, is plotted as a function of the alternation rate J'/J . We set the antiferromagnetic coupling $J = 1$ and change J' . In the inset, the second-order derivative of the groundstate energy exhibits a singular behavior as J'/J approaches 1, which implies that the system undergoes a continuous (a second-order) phase transition across the critical point $J'/J = 1$.

To understand more the critical behavior of the alternating Heisenberg chain in the view of how a bond-dimerized

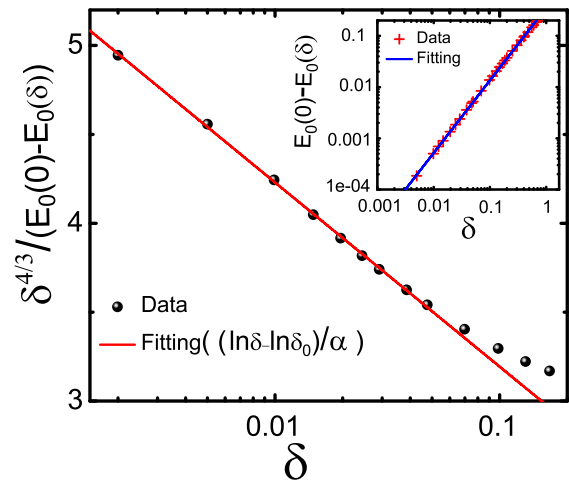


FIG. 3: (Color online) Estimation of the constants α and δ_0 from iMPS data. In the inset, $E_0(0) - E_0(\delta)$ as a function of δ is shown.

Heisenberg chain approaches the uniform limit ($J' = J$) in our iMPS approach, we also calculate the groundstate by using the Hamiltonian $H = \tilde{J} \sum_i (1-\delta) \vec{S}_{2i-1} \cdot \vec{S}_{2i} + (1+\delta) \vec{S}_{2i} \cdot \vec{S}_{2i+1}$, written in terms of the dimerization parameter δ . Here, $\tilde{J} = (J + J')/2$ and $\delta = (J' - J)/(J' + J)$ with $0 \leq \delta \leq 1$. In the Table I, a comparison between the groundstate energies E_0 from DMRG³⁸ and our iMPS approach is made for $\tilde{J} = (J + J')/2 = 1$ and the truncation dimension $\chi = 56$. Note that our iMPS groundstate energies agree very well with those from DMRG.

By virtues of a field theoretical approach, Black and Emery³⁶ have related the critical behavior to the four-state Potts model and found that the energy per site follows a power law with a logarithmic correction, i.e., $E_0(0) - E_0(\delta) \approx \alpha \delta^{4/3} / (\ln \delta - \ln \delta_0)$ with the numerical fitting constants $\alpha \approx -2.2$ and $\delta_0 \approx 110$. By using DMRG, Papenbrock *et al.*³⁹ have also found that a power law ($\propto \delta^{1.45}$) is quite well in the range of $0.008 \leq \delta \leq 0.1$, while logarithmic correction is need for small δ . From our iMPS representation, in Fig. 3, we plot the energy per site $E_0(\delta)$ with the dimerization parameter δ for $\tilde{J} = 1$. $E_0(0) = 1/4 - \ln 2$ is corresponding to the uniform limit. Figure 3 shows the power law behavior with the loga-

TABLE I: Ground state energy per site E_0

Dimerization δ	DMRG E_0^a	iTEBD $E_0(\chi = 56)$
0.000	-0.443147 ^b	-0.443146
0.001	-0.443166	-0.443165
0.002	-0.443196	-0.443197
0.005	-0.443333	-0.443333
0.010	-0.443655	-0.443655
0.020	-0.444537	-0.444537
0.050	-0.448374	-0.448376
0.100	-0.457246	-0.457246
1/3	-0.517954	-0.517954

^aRef. 38.

^bExact solution $E_0 = -\ln 2 + 1/4$ given by Bethe Ansatz.

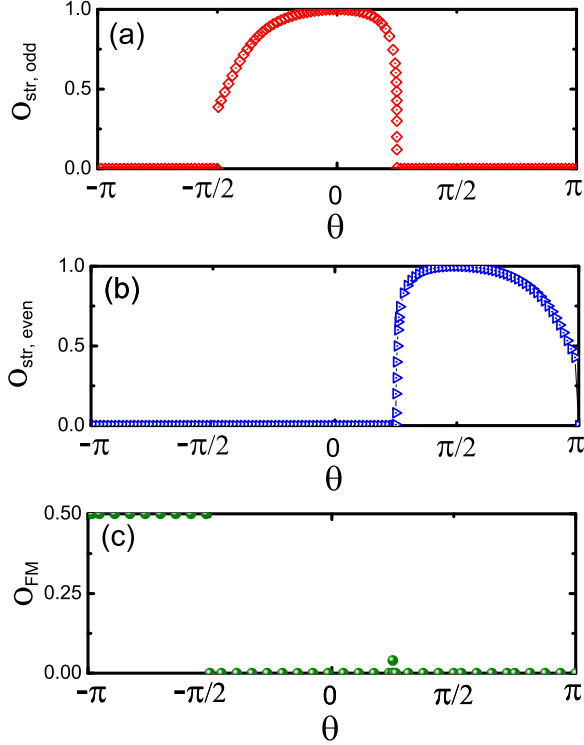


FIG. 4: (Color online) String order parameters $O_{str,odd/even}$ and ferromagnetic order parameter O_{FM} as a function of θ with $J = \cos \theta$ and $J' = \sin \theta$.

rithmic correction, $E_0(0) - E_0(\delta) \approx \alpha \delta^{4/3} / (\ln \delta - \ln \delta_0)$ with the numerical fitting constants $\alpha \approx -2.21$ and $\delta_0 \approx 114$.

III. TOPOLOGICAL QUANTUM PHASE TRANSITION

In the antiferromagnetic Heisenberg Hamiltonian of Eq. (1) with the bond alternation, the transition between the two dimerized states at $J'/J = 1$ does not involve any change of symmetry although the second derivative of the groundstate energy exhibits its singular behavior indicating phase transition in Fig. 3. The absence of any explicit change of symmetry implies no local order parameters characterizing each phase. However, it manifests as a change of topological order, i.e., string order. To see this, let us introduce two string order parameters based on the bond alternation:

$$O_{str,even}^\alpha = \lim_{|i-j| \rightarrow \infty} \left(-4 \langle S_{2i}^\alpha \exp[i\pi \sum_{k=2i+1}^{2j-2} S_k^\alpha] S_{2j-1}^\alpha \rangle \right), \quad (2a)$$

$$O_{str,odd}^\alpha = \lim_{|i-j| \rightarrow \infty} \left(-4 \langle S_{2i+1}^\alpha \exp[i\pi \sum_{k=2i+2}^{2j-1} S_k^\alpha] S_{2j}^\alpha \rangle \right), \quad (2b)$$

where $\alpha = x, y,$ and z . Due to the $SU(2)$ rotationally invariant ground states, $O_{str}^x = O_{str}^y = O_{str}^z$. From our iMPS ground-wavefunction, we directly calculate the defined string orders. In Fig. 4, the order parameters are displayed as a function of the angle variable $\theta = \tan^{-1} J'/J$. As we mentioned, the string

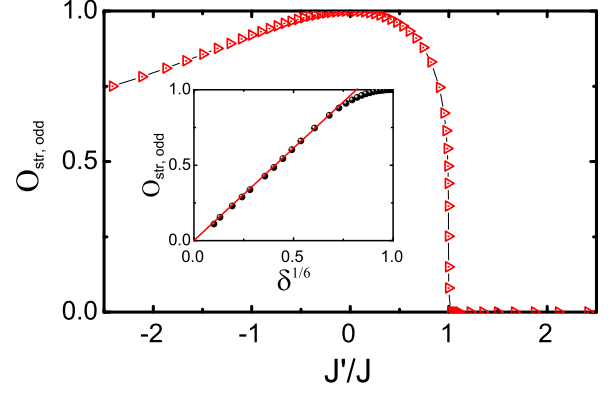


FIG. 5: (Color online) String order parameter $O_{str,odd}$ as a function of J'/J with $J = 1$. In the inset, the string order parameter $O_{str,odd}$ is plotted as a function of $\delta^{1/6}$. The straight line, as a guide of eye, is also drawn.

orders are the saturated values of string correlations for a large lattice distance. Figure 4 clearly shows that the odd string order is finite in the $-\pi/2 < \theta < \pi/4$ phase and zero otherwise, while the even string order is finite in the $\pi/4 < \theta < \pi$. These results imply that each system parameter range can be characterized by each long-range string order. Also, as the system parameter crosses the critical point $J' = J$, the system undergoes a TQPT between the two topologically ordered phases. Similar to the spin-1 Heisenberg chain understood by the hidden $Z_2 \otimes Z_2$ breaking symmetry^{23,40}, a similar hidden symmetry breaking may occur for each phase. Further, we plot the string order parameter $O_{str,odd}$ as a function of J' with $J = 1$ in Fig. 5. In the inset of Fig. 5, the string order parameter $O_{str,odd}$ is plotted as a function of the dimerization parameter δ . Note that the string order parameter $O_{str,odd}$ scales as $\delta^{1/6}$ ²⁷. As a result, the critical exponent is given as $\beta = 1/12$ via $O_{str,odd} \propto \delta^{2\beta}$ ³². Hence, the TQPT is in the same universality class with the Gaussian phase transition.

When the θ approaches $-\pi/2$ or π , the system can be regarded as an effective spin-1 antiferromagnetic Heisenberg chain because of the strong odd- or even-bond dimerizations. In these limits, the numerical values of our string orders $O_{str,odd/even} = 0.3873$ become very close to the results, for the antiferromagnetic spin-1 Heisenberg chain, $O_{str}^{S=1} = 0.37434447$ from the iMPS approach³⁰ and $O_{str}^{S=1} = 0.37432509$ from the DMRG method⁴¹. For $-\pi < \theta < -\pi/2$ ($J' < 0$ and $J < 0$), both the odd and even string orders become zero, while the ferromagnetic local order $O_{FM} = \langle S_i \rangle$ become finite, which indicates that the system is in the ferromagnetic phase. In the magnetization in Fig. 4, one may notice a non-zero value of the local magnetization $\langle S_i \rangle$ at $\theta = \pi/4$, i.e., an isotropic Heisenberg chain that should have zero magnetization. The non-zero value of the magnetization at $\theta = \pi/4$ is due to finite truncation dimension χ . However, it scales down to zero in the limit of infinite truncation dimension, i.e., the thermodynamic limit⁴².

Actually, Hida²⁷ introduced a similar string order parameter to argue a crossover between a Haldane-gap phase and

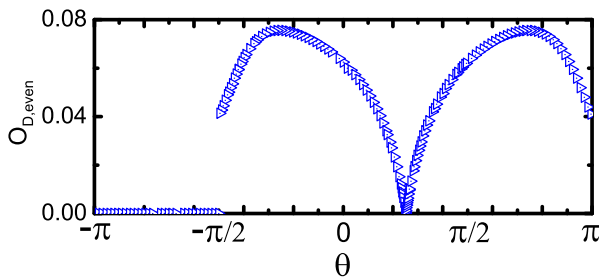


FIG. 6: (Color online) Dimer orders $O_{D,even}$ as a function of θ with $J = \cos \theta$ and $J' = \sin \theta$.

a ‘dimer phase’ in the spin-1/2 bond alternating Heisenberg chain for $J > J'$. However, this ‘dimer phase’ is originated from the symmetry of the Hamiltonian rather than a broken symmetry of groundstate because both the Hamiltonian and its groundstate possess the same symmetry, i.e., two-site translational invariance. In this sense, Hida has found the existence of a topological order for $J' > J$ in the spin-1/2 bond alternating Heisenberg chain for $J > J'$. However, for $J > J'$, no crossover happens in the system because his ‘dimer phase’ might be rather a ‘dimerized state’ due to the bond alternation. To make this point clearer, we calculate the odd- and even- dimer orders defined by

$$O_{D,even} = \lim_{|i-j| \rightarrow \infty} \langle O_D(2i)O_D(2j) \rangle, \quad (3a)$$

$$O_{D,odd} = \lim_{|i-j| \rightarrow \infty} \langle O_D(2i+1)O_D(2j) \rangle, \quad (3b)$$

where $O_D(i) = \vec{S}_i \cdot \vec{S}_{i+1} - \vec{S}_{i+1} \cdot \vec{S}_{i+2}$. In our system, we calculate the even- and odd- dimer orders $O_{D,odd} = -O_{D,even}$. In Fig. 6, the even-dimer order is displayed as a function of the angle variable θ . Both the odd- and even-dimer orders are finite in the two Haldane phases, which implies that the two Haldane phases cannot be distinguished by the dimer orders although both the odd- and even-dimer orders disappear at the critical point $\theta = \pi/4$. These disappearances of the dimer orders at the critical point are originated from the symmetry of the Hamiltonian because the Hamiltonian is one-site translational invariance and its groundstate has the same symmetry of the one-site translation invariance. Consequently, the dimer orders are not the order parameters characterizing the two Haldane phases although the dimer orders exist in the two Haldane phases. Hence, the two long-range string orders characterize the two Haldane phases, respectively, and the TQPT occurs between the two Haldane phases.

IV. VON NEUMANN ENTROPY AND CENTRAL CHARGE

At a quantum critical point, characteristic common singular behaviors of thermodynamics properties, depending only on few features such as dimensionality and symmetry, allow us to classify quantum phase transitions by using the concept of the universality classes, i.e., a type of quantum phase transition. Especially, the central charge⁴³ can be used to classify a universality class of the TQPT at $J'/J = 1$. In the

iMPS representation, at a quantum critical point, one can obtain the central charge c via a so-called finite-entanglement scaling exponent κ numerically from the unique behaviors of the correlation length $\xi = a\chi^\kappa$ and the von Neumann entropy $S = (c\kappa/6) \log_2 \chi$ ⁴⁴. Here, a and χ are a numerical fitting constant and the truncation dimension, respectively. Thus, in order to get more insight on the TQPT, we will discuss the von Neumann entropy and the central charge at $J'/J = 1$ in this section.

Actually, the von Neumann entropy can quantify quantum entanglement as a good measure of bipartite entanglement between two subsystems of a pure state^{45,46}. In our iMPS representation, the spin chain can be partitioned into the two parts denoted by the left semi-infinite chain L and the right semi-infinite chain R . The von Neumann entropy is defined as $S = -\text{Tr} \varrho_L \log_2 \varrho_L = -\text{Tr} \varrho_R \log_2 \varrho_R$ in terms of the reduced density matrix ϱ_L or ϱ_R of the subsystems L and R . The von Neumann entropy for the semi-infinite chains L or R can be expressed as

$$S_i = - \sum_{\alpha=1}^{\chi} \lambda_{i,\alpha}^2 \log_2 \lambda_{i,\alpha}^2, \quad (4)$$

where $\lambda_{i,\alpha}$'s are diagonal elements of the matrix λ that could be directly obtained in the iMPS representation. This is because, when one partitions the two semi-infinite chains $L(-\infty, \dots, i)$ and $R(i+1, \dots, \infty)$, one gets the Schmidt decomposition $|\Psi\rangle = \sum_{\alpha=1}^{\chi} \lambda_{i,\alpha} |\phi_L\rangle |\phi_R\rangle$. From the spectral decomposition, $\lambda_{i,\alpha}^2$ are actually eigenvalues of the reduced density matrices for the two semi-infinite chains L and R . In our two-site translational invariant iMPS representation, there are two Schmidt coefficient matrices λ_A and λ_B that describe two possible ways of the partitions, i.e., one is on the odd sites, the other is on the even sites. From the λ_A and λ_B , one can obtain the two von Neumann entropies depending on the odd- or even-site partitions.

In Fig. 7 (a), we plot the von Neumann entropies S_{odd} and S_{even} as a function of the angle variable $\theta = \tan^{-1} J'/J$. Both the entropies for odd and even bonds show their singular behaviors at the same values $\theta = -\pi/2, \pi/4$, and π . Note that the singular behaviors of the von Neumann entropies correspond to the quantum phase transition points from the order parameters in Fig. 4. Hence, the von Neumann entropies give the same phase diagram from the order parameters.

In Fig. 7 (b) and (c), the correlation length ξ and the von Neumann entropy S are plotted as a function of the truncation dimension χ at the critical point $\theta = \pi/4$ ($J'/J = 1$). The truncation dimensions χ are taken from 16 to 64. It is shown that both the correlation length ξ and the von Neumann entropy S diverge as the truncation dimension χ increases. From a power-law fitting on the correlation length ξ , we have $\kappa = 1.336$ and $a = 0.255$. As shown in Fig. 7 (c), our numerical result demonstrates a linear scaling behavior, which gives a central charge $c \approx 1.004$ with $\kappa = 1.336$. Our central charge is close to the exact value $c = 1$ predicted by conform field theory for an isotropic antiferromagnetic Heisenberg chain. Consequently, the TQPT between the odd- and the even- Haldane phases at $J'/J = 1$ is a Gaussian transition which is

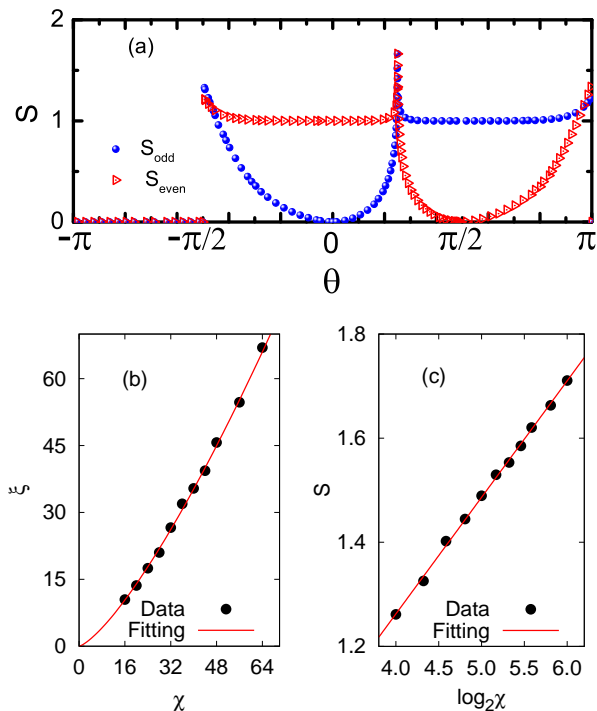


FIG. 7: (Color online) (a) Von Neumann entropies S_{even} and S_{odd} as a function of the parameter θ . The von Neumann entropies for odd- and even-bonds show a peak at $\theta = \pi/4$ and discontinue at $\theta = -\pi/2, \pi$. (b) Correlation length ξ as a function of the truncation dimension χ at the critical point $\theta = \pi/4$. The power curve fitting $\xi = a\chi^\kappa$ yields $a = 0.255$ and $\kappa = 1.336$. (c) Scaling of the von Neumann entropy S with the truncation dimension χ at the critical point $\theta = \pi/4$, i.e., $J' = J$ corresponding to the conventional spin-1/2 AF isotropic Heisenberg chain. For κ from (b), the linear fitting $S = (c\kappa/6)\log_2 \chi + b$ yields $b = 0.369$ and the central charge $c \approx 1.004$.

characterized by a central charge $c = 1$ and the occurrence of a phase transition between two gapful phases. This result is consistent with the classification of the TQPT from the critical exponent $\beta = 1/12$.

V. FIDELITY PER LATTICE SITE

As we discussed in the previous section, the von Neumann entropy, as an entanglement measure, can detect the topological phase transition at $J'/J = 1$. In this section, we study a fidelity per site as another universal indicator for quantum phase transition. From our iMPS groundstate wavefunction $|\Psi(\theta)\rangle$ in terms of the angle variable $\theta = \tan^{-1} J'/J$, one can define a fidelity $F(\theta', \theta) = |\langle \Psi(\theta') | \Psi(\theta) \rangle|$ between the groundstate wavefunctions for two different control parameters θ and θ' . A fidelity per lattice site (FLS)⁴⁷ d can be defined as

$$\ln d(\theta', \theta) = \lim_{N \rightarrow \infty} \frac{\ln F(\theta', \theta)}{N}, \quad (5)$$

where N is the system size. In Fig. 8, the FLS $d(\theta', \theta)$ is plotted in the two dimensional control parameter space. The three

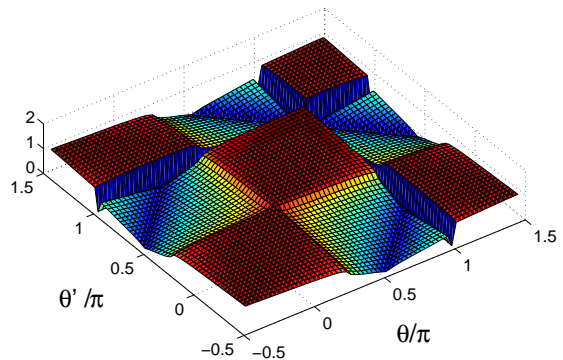


FIG. 8: (Color online) Fidelity per site $d(\theta', \theta)$ surface as a function of two parameter θ' and θ for a bond alternating Heisenberg chain with $J = \cos \theta$ and $J' = \sin \theta$.

singular points $(\theta', \theta) = (\pi/4, \pi/4)$, $(-\pi/2, -\pi/2)$ and (π, π) are observed on the FLS surface, which indicates that there occur quantum phase transitions when control parameters across these values. The continuous behavior of the FLS function across the “pinch” point $(\theta', \theta) = (\pi/4, \pi/4)$ implies that a continuous quantum phase transition occurs for the topological phase transition. The discontinuous behaviors of the FLS function at two other points are corresponding to the first-order quantum phase transitions⁴⁷. The pinch points of the FLS correspond to the quantum phase transition points from the order parameters in Fig. 4 and the von Neumann entropies in Fig. 7(a). The FLS gives the same phase diagram from the order parameters and the von Neumann entropy. Hence, it is shown that a TQPT can be detected by FLS.

VI. CONCLUSION

Quantum phase transitions have been investigated systematically in a spin-1/2 bond-alternating Heisenberg chain by using the iMPS representation with the iTEDB method. By calculating the odd- and even-string orders and the ferromagnetic order, the three phases, i.e., the odd- and even-Haldane phases and the ferromagnetic phases, were found in the plane of the bond-alternating interactions. The TQPT between the odd- and even-Haldane phases was classified as a Gaussian-type phase transition from the central charge at the critical point and the critical exponent of the string orders. Also, it was clearly shown that the FLS and the von Neumann entropy can detect the TQPT.

Acknowledgments

We thank Huan-Qiang Zhou and Jin-Hua Liu for helpful discussions. This work was supported by the Fundamental Research Funds for the Central Universities (Project No. CD-JZR10100027) and the NSFC under Grant No.11104362.

- * Electronic address: sycho@cqu.edu.cn
- ¹ L. D. Landau and E. M. Lifschitz, *Statistical Physics*, Course of Theoretical Physics Vol. 5 (Pergamon, London, 1958).
 - ² P. W. Anderson, *Basic Notions of Condensed Matter Physics* (Addison-Wesley, Reading, MA, 1997).
 - ³ S. Coleman, *An Introduction to Spontaneous Symmetry Breakdown and gauge Fields, Laws of Hadronic Matter*, edited by A. Zichichi (Academic, New York, 1975).
 - ⁴ K. V. Klitzing, G. Dorda, and M. Pepper, Phys. Rev. Lett. **45**, 494 (1980).
 - ⁵ X.-G. Wen, Phys. Rev. B **40**, 7387 (1989).
 - ⁶ X.-G. Wen, Phys. Rev. Lett. **48**, 13749 (1993); X.-G. Wen, Phys. Rev. B **65**, 165113 (2002).
 - ⁷ A. Y. Kitaev, Ann. Phys. (NY) **303**, 2 (2003).
 - ⁸ S. Trebst, P. Werner, M. Troyer, K. Shtengel, and C. Nayak, Phys. Rev. Lett. **98**, 070602 (2007).
 - ⁹ A. Hama and D.A. Lidar, Phys. Rev. Lett. **100**, 030502 (2008).
 - ¹⁰ C. Castelnovo and C. Chamon, Phys. Rev. B **76**, 174416 (2007).
 - ¹¹ X.-Y. Feng, G.-M. Zhang, and T. Xiang, Phys. Rev. Lett. **98**, 087204 (2007).
 - ¹² H. D. Chen and Z. Nussinov, J. Phys. A: Math. Theor. **41**, 075001 (2008).
 - ¹³ J. Yu, S.-P. Kou, and X.-G. Wen, Europhys. Lett. **84**, 17004 (2008).
 - ¹⁴ J. Vidal, R. Thomale, K. P. Schmidt, and S. Dusuel, Phys. Rev. B **80**, 081104 (2009).
 - ¹⁵ D. C. Tsui, H. L. Stormer, and A. C. Gossard, Phys. Rev. Lett. **48**, 1559 (1982).
 - ¹⁶ R. B. Laughlin, Phys. Rev. Lett. **50**, 1395 (1983).
 - ¹⁷ F. D. M. Haldane, Phys. Lett. A **93**, 464 (1983).
 - ¹⁸ V. Kalmeyer and R. B. Laughlin, Phys. Rev. Lett. **59**, 2095 (1987).
 - ¹⁹ X.-G. Wen, F. Wilczek, and A. Zee, Phys. Rev. B **39**, 11413 (1989).
 - ²⁰ N. Read and S. Sachdev, Phys. Rev. Lett. **66**, 1773 (1991).
 - ²¹ X.-G. Wen, Phys. Rev. B **44**, 2664 (1991).
 - ²² R. Moessner and S. L. Sondhi, Phys. Rev. Lett. **86**, 1881 (2001).
 - ²³ M. den Nijs and K. Rommelse, Phys. Rev. B **40**, 4709 (1989).
 - ²⁴ H. Tasaki, Phys. Rev. Lett. **66**, 798 (1991).
 - ²⁵ F. C. Alcaraz and Y. Hatsugai, Phys. Rev. B **46**, 13914 (1992).
 - ²⁶ A. K. Kolezhuk and U. Schollwöck, Phys. Rev. B **65**, 100401 (2002).
 - ²⁷ K. Hida, Phys. Rev. B **45**, 2207 (1992).
 - ²⁸ H.-H. Hung and C.-D. Gong, Phys. Rev. B **71**, 13914 (2005).
 - ²⁹ S. Yamamoto, Phys. Rev. B **55**, 3603 (1997).
 - ³⁰ Y. H. Su, S. Y. Cho, B. Li, H. L. Wang, and H.-Q. Zhou, J. Phys. Soc. Jpn. **81**, 074003 (2012).
 - ³¹ S. R. White, Phys. Rev. B **53**, 52 (1996); G. Fáth, Ö. Legeza, and J. Sólyom, Phys. Rev. B **63**, 134403 (2001); M. Nakamura and S. Todo, Phys. Rev. Lett. **89**, 077204 (2002); H.-H. Hung, C. D. Gong, Y.-C. Chen, and M.-F. Yang, Phys. Rev. B **73**, 224433 (2006); F. Anfuso and A. Rosch, Phys. Rev. B **76**, 085124 (2007) E. H. Kim, Ö. Legeza, and J. Sólyom, Phys. Rev. B **77**, 205121 (2008); S. H. Li, Q. Q. Shi, Y. H. Su, J. H. Liu, Y. W. Dai, and H.-Q. Zhou, Phys. Rev. B **86**, 064401 (2012).
 - ³² D. G. Shelton, A. A. Nersisyan, A. M. Ysvelik Phys. Rev. B **53**, 8521 (1996).
 - ³³ V. O. Garlea, A. Zheludev, L. P. Regnault, J. H. Chung, Y. Qiu, M. Boehm, K. Habicht, and M. Meissner, Phys. Rev. Lett. **100**, 037206 (2008).
 - ³⁴ G. Vidal, Phys. Rev. Lett. **91**, 147902 (2003).
 - ³⁵ G. Vidal, Phys. Rev. Lett. **98**, 070201 (2007).
 - ³⁶ J. L. Black and V. J. Emery, Phys. Rev. B **23**, 429 (1981).
 - ³⁷ T. Barnes, J. Riera, and D. A. Tennant, Phys. Rev. B **59**, 11384 (1999).
 - ³⁸ M. Kumar, S. Ramasesha, D. Sen, and Z. G. Soos, Phys. Rev. B **75**, 052404 (2007).
 - ³⁹ T. Papenbrock, T. Barnes, D. J. Dean, M. V. Stoitsov, and M. R. Strayer, Phys. Rev. B **68**, 024416 (2003).
 - ⁴⁰ M. Oshikawa, J. Phys. Condens. Matter **4**, 7469 (1992).
 - ⁴¹ S. R. White and D. A. Huse, Phys. Rev. B **48**, 3844 (1993).
 - ⁴² H.-L. Wang, J.-H. Zhao, and H.-Q. Zhou, J. Stat. Math. Theor. **44**, 392002 (2011).
 - ⁴³ P. Calabrese and J. Cardy, J. Phys. A: Math. Theor. **42**, 504005 (2009); J. Cardy, *Scaling and Renormalization in Statistical Physics*, (Oxford, University of Oxford, 1996).
 - ⁴⁴ L. Tagliacozzo, T. R. de Oliveira, S. Iblisdir and J. I. Latorre, Phys. Rev. B **78**, 024410(2008); F. Pollmann, S. Mukerjee, A. Turner and J. E. Moore, Phys. Rev. Lett. **102**, 255701 (2009); G. Vidal, J. I. Latorre, E. Rico and A. Kitaev, Phys. Rev. Lett. **90**, 227902 (2003).
 - ⁴⁵ A. Osterloh, L. Amico, G. Falci, and R. Fazio, Nature (London) **416**, 608 (2002).
 - ⁴⁶ L. Amico, R. Fazio, A. Osterloh, and V. Vedral, Rev. Mod. Phys. **80**, 517 (2008).
 - ⁴⁷ H.-Q. Zhou and J.P. Barjaktarevič, J. Phys. A: Math. Theor. **41**, 412001(2008); H.-Q. Zhou, R. Orús, and G. Vidal, Phys. Rev. Lett. **100**, 080601 (2008).